Supporting Information

Johmura et al. 10.1073/pnas.1106223108

SI Materials and Methods

Plasmid Construction. To generate lentivirus-based sh-Nedd1 (pKM1287) or sh-Hice1 (pKM2720) constructs, an oligonucleotide containing the nucleotides 255–273 of Nedd1 (forward 5′-CCGG**GCAGACATGTGTCAATTTA**CTCGAG**TAAATTGACACATGTCTGC**TTTTTG -3′ and reverse 5′-AATTCAAAAA**GCAGACATGTGTCAATTTA**CTCGAG**TAAATTGACACATGTCTGC** -3′; targeting sequence in boldface type) or the nucleotides 492–510 of Hice1 (forward 5′-CCGG**GAACAATCTTGCTGAGTTT**CTCGAG**AAACTCAGCAAGATTGTTC**TTTTTG -3′ and reverse 5′-AATTCAAAAA**GAACAATCTTGCTGAGTTT**CTCGAG**AAACTCAGCAAGATTGTTC** -3′; targeting sequence in boldface type) was annealed and inserted into pLKO.1-puro vector (a gift of S.A. Stewart and P.A. Sharp, Massachusetts Institute of Technology, Cambridge, MA) digested with AgeI/EcoRI. All of the target sequences for lentivirus-based sh-RNAs are summarized in Table S1.

To construct the plasmid, pcDNA3-ZZ-TEV-Nedd1 (pKM1963), the BglII/SalI fragment containing the full-length cDNA from a pCMV-Nedd1-myc-His construct bearing silent mutations against sh-Nedd1 (a gift of Jens Lüders, Institute for Research in Biomedicine, Barcelona, Spain) was inserted into a pcDNA3-ZZ-TEV vector (a gift of Myung Hee Park, National Institutes of Health, Bethesda, MD) digested with BamHI/XhoI. The ZZ tag is a derivative of the *Staphylococcus* protein A that has a high affinity to IgG. The TEV sequence provides a cleavage site for a highly site-specific protease found in the tobacco etch virus (TEV). The Nedd1 mutant constructs, pcDNA3-ZZ-TEV-Nedd1-S460A T550A (pKM1964), -S411A (pKM2659), -S460A (pKM2660), and -T550A (pKM2661) were generated by a PCR-based, site-directed mutagenesis.

To create a lentiviral construct expressing Nedd1-myc-His (pKM1917), a BglII/NotI (end filled) fragment from the pCMV-Nedd1-myc-His construct described above was inserted into pHR′-CMV-SV-puro vector (a gift of Chou-Zen Giam, Uniformed Services University of the Health Sciences, Bethesda, MD) digested with BamHI/SalI (end filled). The Nedd1 mutant constructs, pHR′-CMV-SV-puro-Nedd1-myc-His-S460A T550A (pKM1927), -S411A (pKM2663), -S460A (pKM2664), and -T550A (pKM2665) were generated by a PCR-based mutagenesis.

The lentiviral construct expressing histone H2B-EGFP (pKM1461) or EB1-EGFP (pKM2416) was generated by inserting a KpnI (end filled)/BamHI (end filled) fragment from pEGFP-N1-Histone H2B (a gift of Keiju Kamijo, Tohoku University Graduate School of Medicine, Miyagi-Ken, Japan) or a BglII/NotI (end filled) fragment from pEGFP-N1-EB1 (a gift of Yasuhiko Terada, Waseda University, Tokyo, Japan), respectively, into pHR′-CMV-SV-puro vector digested with BamHI (end filled) or BamHI/SalI (end filled).

The pGEX4T-1-Nedd1 construct was kindly provided by Kunsoo Rhee (Seoul National University, Seoul, South Korea). The pGEX4T-1-Nedd1-S460A T550A (pKM1930), -S460A (pKM2666), and -T550A (pKM2667) were constructed by a PCR-based mutagenesis. The pGEX4T-2-Cep27 (pKM1189), pGEX6P-2-CCDC5 (pKM1605), -C14ORF94 (pKM1607), -Hice1 (pKM1609), -UCHL5IP (pKM1611), and pGEX6P-1-FAM29A (pKM1613) were constructed by inserting an EcoRV/NotI fragment containing the full-length cDNA into the respective vector digested with SmaI/NotI. Generation of the EGFP-Hice1 (pKM1721) construct was done by inserting a BamHI/NotI fragment containing the full-length cDNA into pShuttle-CMV-EGFP vector digested with BglII/NotI.

Construction of the *HICE1* allele bearing silent mutations against sh-Hice1 was performed by a PCR-based mutagenesis. The silent mutant allele contains 5′-GAA**T**AATCTG**GC**CGA**A**-TTT-3′ (from nucleotides 492–510) (silent mutations are indicated in boldface type). To create a lentiviral construct expressing Hice1 (pKM2708), a BglII/XhoI fragment containing the full-length cDNA bearing silent mutations against sh-Hice1was inserted into pHR′-CMV-SV-puro vector digested with BamHI/SalI. The Hice1 mutant constructs, pHR′-CMV-SV-puro-Hice1-S19A S20A S21A (pKM2709), -S69A (pKM2710), -T122A S124A (pKM2711), -S129A T130A S131A S133A (pKM2712), -S139A (pKM2713), -S143A (pKM2714), -S151A (pKM2715), -S220A (pKM2716), -T235A T242A T243A (pKM2717), -T238A (pKM2718), -S311A (pKM2719), -S129A T130A S131A S133A S143A S151A (pKM2727), or -S129D T130D S131D S133D S143D S151D (pKM2728) were produced using a PCR-based mutagenesis as above.

Cell Culture, Transfection, and Virus Generation and Infection. Cell lines were cultured as recommended by American Type Culture Collection. Cells were trapped in S phase or in prometaphase by treating them with 2.5 mM of thymidine (Sigma) or 200 nM of nocodazole (Sigma), respectively, for 20 h. For double-thymidine block and release experiments, HeLa cells were arrested for 16 h with 2.5 mM thymidine with a 9-h release interval between the thymidine treatments. To inhibit Cdc2, 200 nM of BMI-1026 (1) was added into the reaction mixture.

Transfection was routinely carried out with Lipofectamine 2000 (Invitrogen). For the production of lentiviruses, transfection was performed by the calcium phosphate coprecipitation method (2). Lentiviruses expressing EGFP-Plk1, histone H2B-EGFP, EB1-EGFP, various Nedd1-myc-His or Hice1 constructs were generated by cotransfecting 293T cells with pHR′-CMVΔR8.2Δvpr, pHR′-CMV-VSV-G (protein G of vesicular stomatitis virus), and the respective pHR′-CMV-SV-puro-based constructs described above.

For the production of sh-RNA lentiviruses, pHR′-CMVΔR8.2Δvpr and pHR′-CMV-VSV-G were cotransfected into 293T cells with pLKO.1-puro-sh-Luciferase (sh-Luc), -sh-Plk1, -sh-Nedd1, or -sh-Hice1. To select a lentivirus-integrated population, HeLa cells infected with indicated viruses were treated with 2 μg/mL of puromycin for 2–3 d.

Antibody Production. Bacterially expressed glutathione *S*-transferase (GST)-fused Nedd1(336–660) (numbers indicate the position of amino acid residues) was purified using glutathione (GSH)-agarose (Amersham Biosciences) and then injected into rabbits to raise polyclonal anti-Nedd1 antisera (Rockland Immunologicals). To affinity purify the anti-Nedd1 antibody, immunized sera were purified using MBP-Nedd1(336-660) immobilized with Affigel-10 (Bio-Rad Laboratories). A rabbit anti–p-S460 monoclonal antibody was developed through National Cancer Institute Office of Science and Technology Partnerships-Epitomics collaboration. Antibodies were raised using synthetic peptides, CSSTSV-LHSpSPLNVFMG-NH_2 (p-S460 is underlined), as immunogens.

Immunoprecipitation, Immunoblotting Analyses, and in Vitro Kinase Assay. Immunoprecipitation was carried out essentially as described previously (3). Briefly, cells were lysed in TBSN buffer [20 mM Tris-Cl (pH 8.0), 150 mM NaCl, 0.5% Nonidet P-40, 5 mM EGTA, 1.5 mM EDTA, 0.5 mM Na3VO4, and 20 mM *p*-nitrophenylphosphate (PNPP)]. The resulting lysates were clar-

ified by centrifugation at 15,000 × *g* for 20 min at 4 °C before immunoprecipitation with the specified antibody. Immunoprecipitated proteins were separated by SDS-polyacrylamide gel electrophoresis (SDS/PAGE), transferred to polyvinylidene difluoride (PVDF) (Immobilon-P; Millipore) membrane, and then detected by immunoblotting with the indicated antibodies using the enhanced chemiluminescence (ECL) detection system (Pierce). All antibodies used in this study are listed in Table S2.

In vitro kinase assays were carried out essentially as described previously (3) in a kinase mixture containing 50 mM Tris-HCl (pH 7.5), 10 mM $MgCl_2$, 5 mM DTT, 2 mM EGTA, 0.5 mM Na_3VO_4, and 20 mM PNPP. Both WT and kinase-inactive forms of HA-Plk1(K82M) (3) and the GST-Cyclin B1/Cdc2 complex (a gift of Helen Piwnica-Worms, Washington University, St. Louis, MO) were purified from Sf9 cells. To examine ATP-dependent generation of the p-S460 epitope, 500 μM of ATP was provided into the reaction.

In Vitro Reconstituted GST–Nedd1 Binding Assay. To investigate whether Cdc2-dependent Nedd1 phosphorylation is sufficient to generate Plk1-binding sites, bead-bound GST–Nedd1 (full-length) purified from *Escherichia coli* BL21(DE3) was first reacted with Sf9-purified, soluble, GST–Cyclin B1/Cdc2 in the presence of 500 μM ATP. The resulting GST–Nedd1 was precipitated, washed in TBSN buffer, and then incubated with a mixture of HeLa lysates expressing FLAG–Plk1 (4), FLAG–Plk2 (5), or FLAG–Plk3 (a gift of Doug Ferris, National Cancer Institute, Frederick, MD). After binding, the GST–Nedd1-associated proteins were precipitated, separated by 8% SDS/PAGE, and then analyzed by immunoblotting analyses.

His-Tag and ZZ-Tag Affinity Purification. For His-tag purification, total cell lysates were prepared from 293T cells transfected with the indicated Nedd1-myc-His constructs, and then subjected to affinity purification with a His-select Nickel Affinity Gel (Sigma). Samples were boiled in sample buffer, separated by 7% SDS/PAGE, and immunoblotted.

For ZZ-tag affinity purification, total cellular lysates were prepared from 293T cells transfected with various ZZ-TEV-Nedd1 constructs and then subjected to affinity purification with a human IgG (Amersham Biosciences) column. After digestion with AcTEV protease (Invitrogen), proteins were eluted with TBSN buffer, separated by 8% SDS/PAGE, and then analyzed by immunoblotting.

Mass Spectrometry Analysis. To determine the in vivo phosphorylation sites on Nedd1 or Hice1, 293T cells were transfected with the ZZ-TEV-Nedd1 construct or the EGFP-Hice1 construct, and treated with 200 nM of nocodazole for 20 h to arrest the cells in prometaphase (the stage where the Nedd1–Plk1 interaction is high). ZZ-Nedd1 or EGFP-Hice1 was immunoprecipitated with a human IgG column (Amersham Biosciences) or with anti-GFP antibody, respectively, and the protein samples were separated by 8% SDS/PAGE. To determine Cdc2 or Plk1-dependent phosphorylation sites in vitro, recombinant GST-Nedd1 or GST-Hice1 was reacted with Cdc2/GST-Cyclin B1 or Plk1 in the presence of excess ATP.

After SDS/PAGE, the proteins were excised from the gel and then subjected to in-gel digestion with trypsin (Promega). The resulting peptides were analyzed using nanoLC-tandem mass spectrometry as described previously (6). Briefly, nanoflow reversed-phase liquid chromatographic separation was coupled online to an LTQ linear ion trap mass spectrometer (Thermo Electron) for MS/MS and MS/MS/MS analysis (nanoLC-MS^2-MS^3). The peptides were separated at a flow rate of ~200 nL/min using a step gradient of 2–42% solvent B (0.1% formic acid in acetonitrile) for 40 min, 42–98% solvent B for 10 min and 98–98% solvent B for 5 min, whereas mobile phase A was 0.1% formic acid in water. The mass spectrometer was operated in a data-dependent mode to sequentially acquire MS, MS^2, and neutral phosphate loss-dependent MS^3 spectra with dynamic exclusion. Normalized collision energy was 35% for both MS^2 and MS^3. The raw MS^2 and MS^3 data were searched using Sequest (Thermo Electron) against a protein database including ZZ-Nedd1 or EGFP-Hice1 to identify phosphopeptides. The identified tryptic phosphopeptides were further subjected to manual validation of the peptide sequence and phosphorylation sites by examining the corresponding MS^2 and/or MS^3 spectra.

GST-PBD Pull-Down, Peptide Binding, and Peptide Competition. GST–PBD and its respective GST–PBD (H538A K540M) phospho-pincer mutant (7) (gifts of Michael B. Yaffe, Massachusetts Institute of Technology, Cambridge, MA) were expressed in *E. coli* BL21(DE3) and purified with GSH-agarose (Sigma). To carry out PBD pull-down assays, ~5 μg of bead-associated GST–PBD or GST–PBD (H538A K540M) ligand was incubated with 1–2 mg of total cellular lysates prepared in TBSN buffer for 1.5 h, and then precipitated. The precipitates were washed with TBSN buffer seven times, separated by SDS/PAGE, and then transferred to PVDF membrane for immunoblotting analyses with the indicated antibodies.

Peptide binding assays were carried out essentially as described previously (8). Briefly, synthesized peptides [p-S63 peptide, C-$(CH2)_6$-IVVSpSCK-NH_2; p-T155 peptide, C-$(CH2)_6$-TNLSSpTPF-NH_2; p-S453 peptide, C-$(CH2)_6$-NPVTSpSTS-NH_2; p-S460 peptide, C-$(CH2)_6$-VLHSpSPL-NH_2; p-T550 peptide, C-$(CH2)_6$-INGSSpTPN-NH_2; underlining indicates the phosphorylated residues] were cross-linked to the beads using SulfoLink coupling gel (Pierce). The resulting immobilized peptides were then incubated with HeLa lysates in TBSN buffer. The HeLa lysates were prepared from cells treated with 200 nM of nocodazole for 20 h to enrich the amount of Plk1. After incubation, precipitates were washed seven times, separated by SDS/PAGE, and then transferred to PVDF membrane for immunoblotting analyses.

To test the ability of the p-S460 peptide and/or the p-T550 peptide to disrupt the interaction between Plk1 and Nedd1, mitotic HeLa lysates were prepared in TBSN buffer and incubated with 100 μg/mL of the indicated phosphopeptides (p-S460 peptide, Ac-VLHSpSPL-NH_2; p-T550 peptide, Ac-INGSSpTPN-NH_2; phosphorylated residues are underlined) or the corresponding non-phospho-peptides for 15 min at 4 °C. The resulting lysates were then subjected to anti-Plk1 immunoprecipitation followed by immunoblotting analyses.

2D Polyacrylamide Gel Electrophoresis. Total cell lysates were prepared with 8 M urea and resolved in a sample buffer for isoelectric focusing (IEF) (9.5 M urea, 2% Nonidet P-40, 2% Ampholine (Pharmacia), and 5% 2-mercaptoethanol). An IEF disk gel (2-mm diameter and 12 cm long) consisted of 9.2 M urea, 4% acrylamide, 0.32% *N*,*N*′- methylenebisacrylamide, 0.1% tetramethylethylenediamine (TEMED), 2% Nonidet P-40, 5% Ampholine, and 0.015% ammonium persulfate. IEF was performed using Protean II Xi Cell (Bio-Rad). The electrode buffer of positive pole (10 mM H_3PO_4) was poured into the lower chamber, and the disk gels were assembled. After sample solutions were applied, 10 μL of a sample protection buffer (9 M urea and 2.5% Ampholine) was put on the sample layer, and electrode buffer of negative pole (20 mM NaOH) was poured into the upper chamber. IEF was carried out at 400 V for 16 h at room temperature. After IEF electrophoresis, disk gels were soaked for 60 min with a 0.25 M Tris-HCl (pH 6.8) buffer containing 2.5% SDS, 5% 2-mercaptoethanol, and 10% glycerol, separated by 8% SDS/PAGE, and then transferred to PVDF membrane for immunoblotting analyses with the Hice1 antibody.

Microtubules Cosedimentation Assay. Total lysates were prepared from HeLa cells arrested with nocodazole for 20 h. The lysates were incubated with 1 mM of GTP and 20 μM of taxol in PME buffer (100 mM Pipes, pH 6.9, 1 mM $MgSO_4$, and 2 mM EGTA) at 37 °C for 30 min. The resulting lysates were underlaid with ~300 μL of 10% sucrose cushion in PME buffer containing 20 μM of taxol and protease inhibitors, and then centrifuged at 45,000 × *g* for 30 min at 37 °C. Following the centrifugation, the resulting supernatants were collected and the pellets containing the assembled MTs were washed three times with PME buffer. Samples were separated by 8% SDS/PAGE and then subjected to immunoblotting analyses with the indicated antibodies.

Indirect Immunofluorescence Microscopy and Quantification. Indirect immunostaining was carried out as described previously (9). All of the appropriate secondary antibodies [Alexa Fluor 488 (green) or Texas red (red)-conjugated antibodies] were purchased from Invitrogen. To stain chromosomes, cells were treated with PBS containing 0.1 μg/mL of 4′,6′-diamidino-2-phenylindole (DAPI) (Sigma). Confocal images were acquired using a Zeiss LSM 510 system mounted on a Zeiss Axiovert 100M microscope (Carl Zeiss MicroImaging). For the quantification of the fluorescence signal intensities, images of unsaturated fluorescence signals were acquired with the same laser intensity at 512 × 512 pixels and 12-bit resolution. Fluorescence intensity for a particular subcellular signal or an entire cell (for the nucleating MT intensity in Fig. 5*C*) was determined after subtraction of the background signal intensity using Zeiss AIM confocal software.

Time-Lapse Microscopy. HeLa cells infected with lentivirus expressing EGFP-histone H2B were cultured on a Lab-Tek chambered coverglass (Nunc), placed on the stage of the Zeiss LSM 510 NLO confocal system (Carl Zeiss MicroImaging) equipped with an environmental chamber (Precision Plastics) providing temperature, humidity, and CO_2 control. Time-lapse images were captured every 4 min with the 488-nm line of an Argon laser. Images were analyzed by using Carl Zeiss AIM software.

HeLa cells stably expressing EB1-EGFP were cultured on a Lab-Tek chambered coverglass and then subjected to Zeiss VivaTome spinning disk microscopy using aperture correlation methodology (Carl Zeiss MicroImaging). Time-lapse images were collected at 1-s intervals with 300-ms exposure time using 63×/1.4 NA objective and HRm Camera Rev.3 14 bit/1.4 megapixel with 1 peltier cooling stage and a filter set of green 494/20 and 536/40 emission (Carl Zeiss MicroImaging). A high-resolution grid was used for maximum resolving power and high light efficiency.

1. Seong YS, et al. (2003) Characterization of a novel cyclin-dependent kinase 1 inhibitor, BMI-1026. *Cancer Res* 63:7384–7391.
2. Chen C, Okayama H (1987) High-efficiency transformation of mammalian cells by plasmid DNA. *Mol Cell Biol* 7:2745–2752.
3. Lee KS, Yuan Y-L, Kuriyama R, Erikson RL (1995) Plk is an M-phase-specific protein kinase and interacts with a kinesin-like protein, CHO1/MKLP-1. *Mol Cell Biol* 15: 7143–7151.
4. Kang YH, et al. (2006) Self-regulated Plk1 recruitment to kinetochores by the Plk1-PBIP1 interaction is critical for proper chromosome segregation. *Mol Cell* 24:409–422.
5. Ma S, Liu MA, Yuan Y-L, Erikson RL (2003) The serum-inducible protein kinase Snk is a G1 phase polo-like kinase that is inhibited by the calcium- and integrin-binding protein CIB. *Mol Cancer Res* 1:376–384.
6. Yu LR, et al. (2007) Improved titanium dioxide enrichment of phosphopeptides from HeLa cells and high confident phosphopeptide identification by cross-validation of MS/MS and MS/MS/MS spectra. *J Proteome Res* 6:4150–4162.
7. Elia AE, et al. (2003) The molecular basis for phosphodependent substrate targeting and regulation of Plks by the Polo-box domain. *Cell* 115:83–95.
8. Yun SM, et al. (2009) Structural and functional analyses of minimal phosphopeptides targeting the polo-box domain of polo-like kinase 1. *Nat Struct Mol Biol* 16:876–882.
9. Seong YS, et al. (2002) A spindle checkpoint arrest and a cytokinesis failure by the dominant-negative polo-box domain of Plk1 in U-2 OS cells. *J Biol Chem* 277: 32282–32293.
10. Lüders J, Patel UK, Stearns T (2006) GCP-WD is a gamma-tubulin targeting factor required for centrosomal and chromatin-mediated microtubule nucleation. *Nat Cell Biol* 8:137–147.
11. Zhang X, et al. (2009) Sequential phosphorylation of Nedd1 by Cdk1 and Plk1 is required for targeting of the gammaTuRC to the centrosome. *J Cell Sci* 122:2240–2251.
12. Zhu H, Fang K, Fang G (2009) FAM29A, a target of Plk1 regulation, controls the partitioning of NEDD1 between the mitotic spindle and the centrosomes. *J Cell Sci* 122:2750–2759.

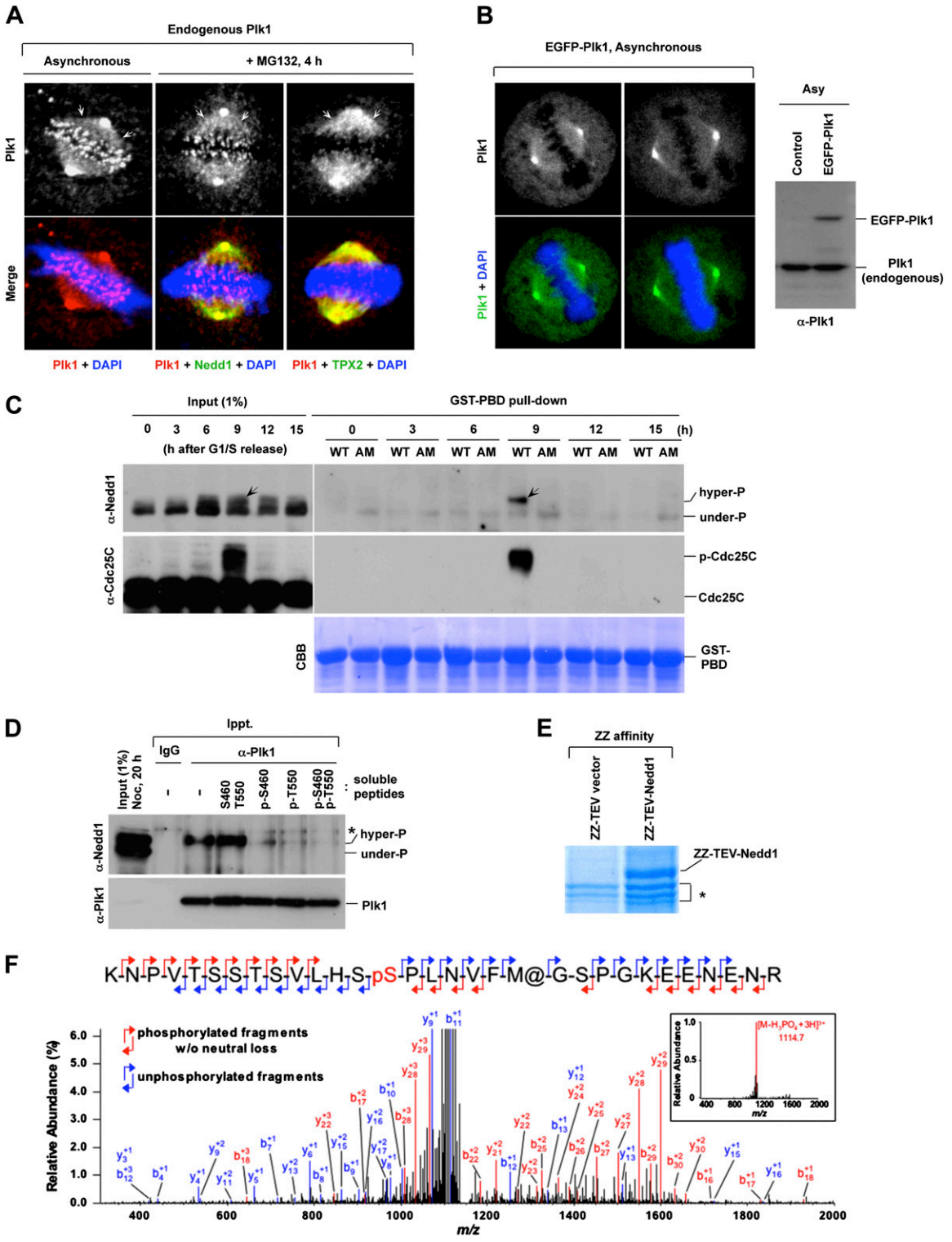

Fig. S1. Subcellular localization of Plk1 and determination of the S460 residue of Nedd1 as a PBD-binding site. (*A* and *B*) Subcellular localization of Plk1 to the mitotic spindles. (*A*) Asynchronously growing HeLa cells were either untreated or treated with MG132 for 4 h to arrest the cells in metaphase. The cells were fixed and immunostained with the indicated antibodies. Arrows, endogenous Plk1 signals at or around the spindles. (*B*) Asynchronously growing (Asy) HeLa cells infected with either control lentivirus or lentivirus expressing EGFP–Plk1 were fixed and stained with DAPI to perform confocal microscopy (*Left*) or harvested and immunoblotted to determine the level of EGFP–Plk1 expression (*Right*). (*C*) Total lysates prepared from HeLa cells releasing synchronously from a G1/S block were subjected to GST–PBD pull-down and immunoblotting analyses. An arrow indicates the hyperphosphorylated form of Nedd1 binding specifically to WT PBD. WT, GST–PBD; AM, GST–PBD (H538A K540M) phosphobinding defective "phospho-pincer" mutant (7). Note that PBD interacts with the hyperphosphorylated Nedd1 at the stage where Cdc2 efficiently generated PBD-binding phospho-Cdc25C (p-Cdc25C), a mitotic phosphatase. (*D*) Anti-Plk1 immunoprecipitation was carried out in the absence or presence of 100 μg/mL of the indicated peptide and analyzed by immunoblotting analyses. Asterisk, a cross-reacting protein. (*E* and *F*) Determination of Nedd1 phosphorylation sites by mass spectrometry analyses. (*E*) 293T cells transfected with control ZZ-TEV vector or ZZ-TEV-Nedd1 were treated with nocodazole for 20 h to enrich mitotic phosphorylation and then subjected to affinity purification using a rabbit IgG

Legend continued on following page

column. Proteins that bound to the column were dissociated by boiling with SDS sample buffer and then separated by 8% SDS/PAGE. An asterisk indicates nonspecific proteins cross-reacting with the column. (*F*) The ZZ-Nedd1 protein excised from the gel in *E* was subjected to tandem mass spectrometry analysis, as described in *Materials and Methods*. The phosphorylation sites were determined by the phosphorylated (red) fragment ions with (w/) or without (w/o) neutral loss of phosphate and unphosphorylated (blue) fragment ions. In addition to the S411 (10) and T550 (11) residues [the amino acid numbering is for Nedd1 isoform b that lacks the less-conserved N-terminal 7 residues found in Nedd1 isoform **a** (10), Nedd1 was phosphorylated at S460 in vivo. The mass spectrometry result that led to the identification of the phosphorylated S460 peptide is shown. @, an oxidated residue; #, alkylated residue.

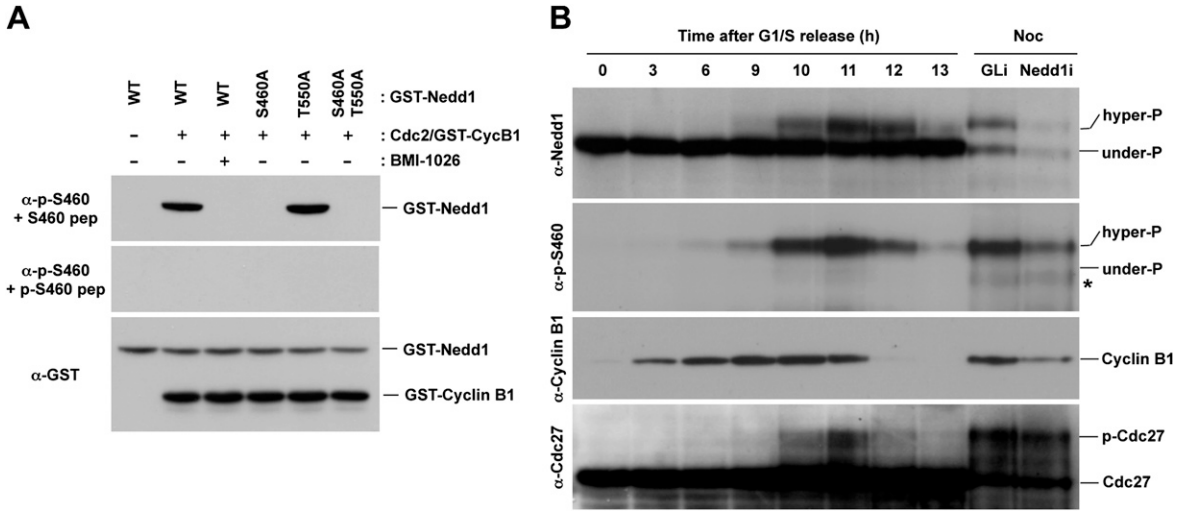

Fig. S2. Generation of the p-S460 epitope at the late stage of the cell cycle. (*A*) Various GST–Nedd1 forms purified from bacterial cells were reacted with purified Cdc2/GST–Cyclin B1 in the presence or absence of a Cdc2 inhibitor, BMI-1026 (1). The resulting samples were separated by SDS/PAGE and immunoblotted. Note that the levels of GST–Cyclin B1 represent the Cdc2/GST–Cyclin B1 complex purified from Sf9 cells using glutathione-agarose beads. (*B*) HeLa cells synchronously releasing from a G1/S block were harvested and subjected to immunoblotting analyses. Anti-Cdc27 immunoblot was carried out to monitor cell cycle progression, while avoiding the size overlap with phosphorylated Nedd1. Arrows, cross-reacting proteins. Note that S460-phosphorylated Nedd1 was detectable at the stage where the phosphorylated form of Cdc27, a Cdc2 substrate, began to appear, indicating that these phosphorylations occur at the time of Cdc2 activation. In addition, the p-S460 epitope was found to be associated with the slow-migrating form of endogenous Nedd1, suggesting that phosphorylation of S460 occurs after S411 phosphorylation.

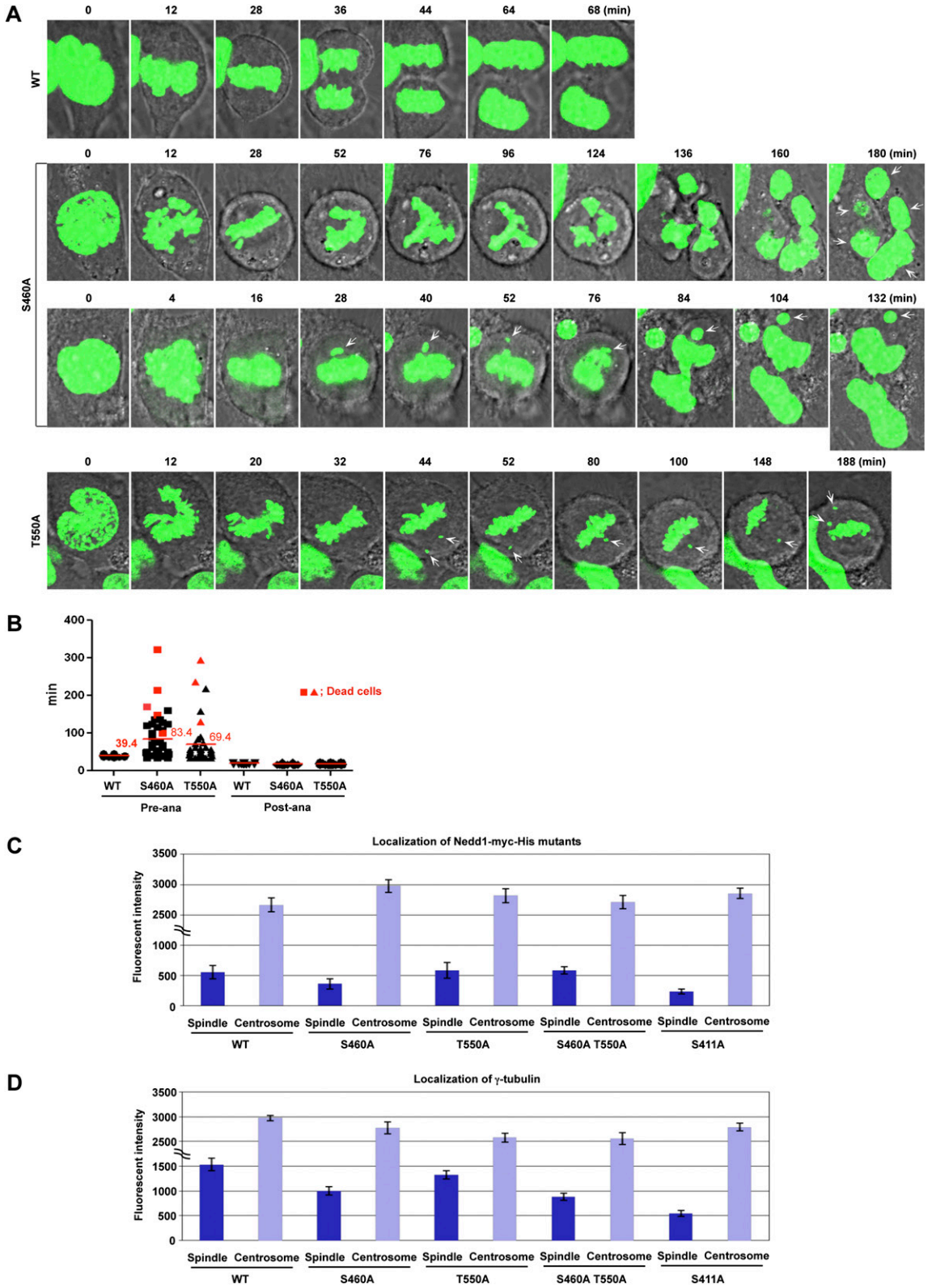

Fig. S3. Differential role of p-S460 or p-T550–dependent Nedd1–Plk1 interaction and requirement of S460 and S411-dependent Nedd1 function for proper localization to the spindle. (*A*) Two distinct defects associated with the loss of p-S460 or p-T550–dependent Nedd1–Plk1 interaction. HeLa cells expressing Nedd1 WT, Nedd1 S460A, or Nedd1 T550A were infected with lentivirus expressing EGFP-histone H2B. The resulting cells were then depleted of endogenous Nedd1 and arrested at the G1/S boundary by double-thymidine treatment. Eight hours after release from the G1/S block, cells were monitored under time-lapse microscopy. Cells expressing WT Nedd1 exhibited normal mitotic progression (first row). However, cells expressing the 460A mutant exhibited a significant preanaphase delay due to the presence of misaligned chromosomes. These cells frequently exhibited micronucleated chromosome morphology (second row), although a fraction of cells with lagging chromosomes (third row) were also apparent. Unlike the 460A-expressing cells, the cells expressing the 550A

Legend continued on following page

mutant did not exhibit a significant level of micronucleated morphology even after a prolonged preanaphase arrest (fourth row). This difference is consistent with the observation that the 460A mutant generates a high level of multipolar chromosome morphologies as shown in Fig. 2*C*. Arrows in the second row point to micronucleated chromosomes. Arrows in the third row indicate a misaligned chromosome that becomes a missegregating chromosome at later stages. Arrows in the fourth row denote misaligned chromosomes that cause a prolonged mitotic arrest. Time in all rows is given in minutes. Cells depicted in Movies S1, S2, S3, and S4). (*B*) The length of time required for preanaphase (Preana) or postanaphase (Postana) progression in *A* was quantified. Red bars with numbers indicate the averages of time length in minutes. Red squares and triangles indicate the cells that exhibited apoptotic cell death after a prolonged mitotic arrest. (*C* and *D*) The actual quantification data of the Nedd1-myc-His and γ-tubulin fluorescence intensities used for the generation of Fig. 2*F*. Quantification of Nedd1-myc-His and γ-tubulin fluorescence intensities for the samples in Fig. 2*E* was carried out as described in *Materials and Methods* ($n > 20$ cells per sample). Relative fluorescence intensities between spindle and centrosomes were determined from each individual cell first and then the resulting numbers were used to generate Fig. 2*F*. Error bars, SD.

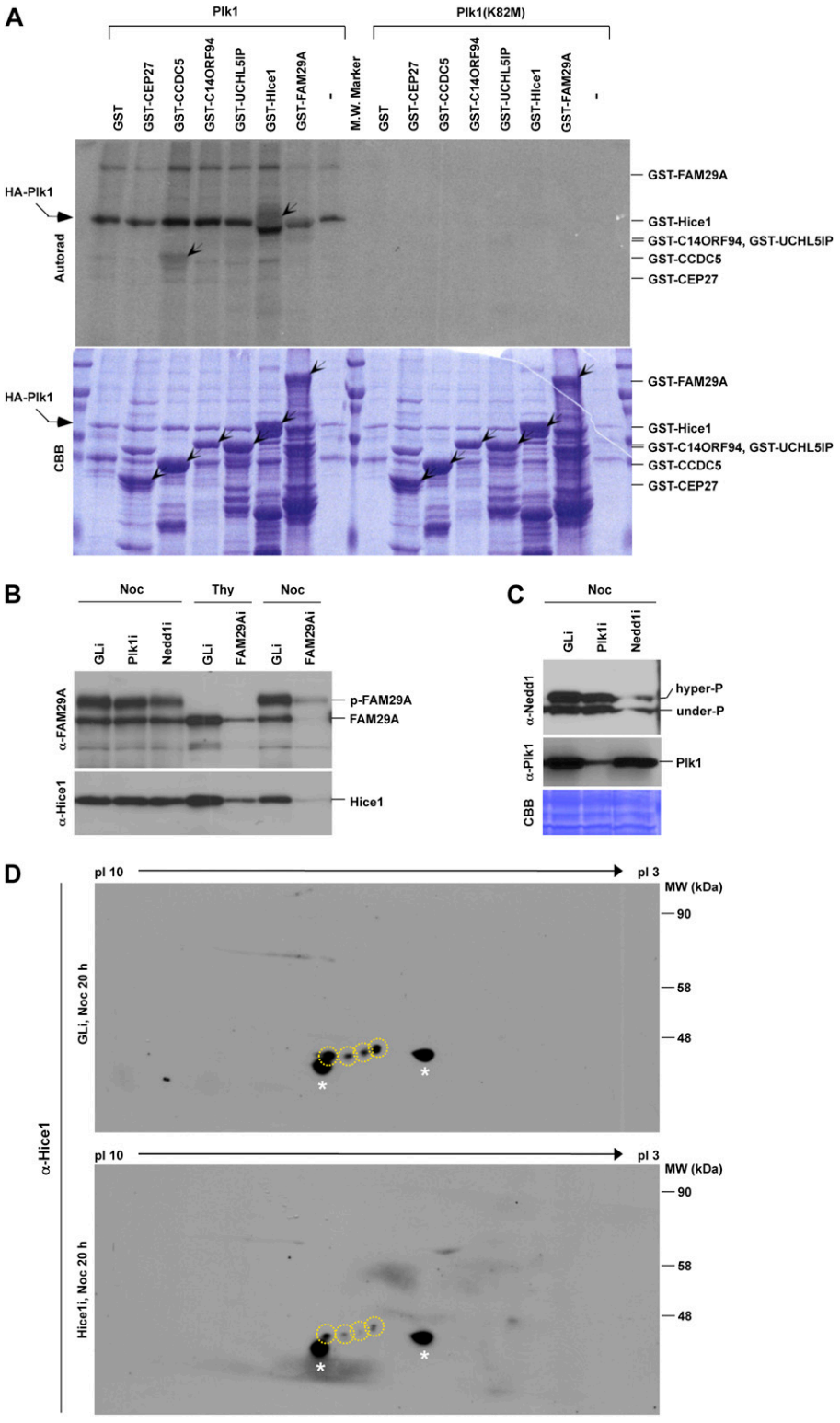

Fig. S4. Plk1-dependent Augmin phosphorylation and 2D gel electrophoresis for Hice1 phosphorylation. (*A*–*C*) Plk1 phosphorylates Hice1 and CCDC5 in vitro, and both Plk1 and Nedd1 are not required for FAM29A phosphorylation in vivo. (*A*) To examine whether Plk1 phosphorylates Augmin subunits in vitro, WT Plk1 or kinase-inactive Plk1 (K82M) (3) was reacted with the indicated GST-fused recombinant proteins purified from *E. coli*. After terminating the reactions, samples were separated by 10% SDS/PAGE, stained with Coomassie (CBB), and then exposed. Arrows in the autoradiogram indicate Hice1 and CCDC5 phosphorylated by Plk1. Arrows in the CBB denote the full-length proteins. Although Plk1 has been suggested as a kinase that regulates FAM29A in a kinase activity-dependent manner (12), Plk1 failed to phosphorylate GST–FAM29A significantly under our conditions. (*B* and *C*) HeLa cells were treated with lentiviruses expressing either control sh-luciferase (GLi), sh-Plk1 (Plk1i), sh-Nedd1 (Nedd1i), or sh-FAM29A (FAM29Ai). The resulting cells were additionally treated with thymidine or nocodazole for 20 h, harvested, and then immunoblotted. (*D*) 2D gel electrophoresis to identify Hice1-specific protein spots. HeLa cells infected with either control sh-luciferase (GLi) (*Upper*) or sh-Hice1 (Hice1i) (*Lower*) were arrested in mitosis by treating the cells with nocodazole for 20 h. Total cellular lysates prepared from the resulting cells were subjected to 2D electrophoresis. The four protein spots whose signals are greatly diminished in Hice1i cells (marked with yellow dotted circles) were identified as phosphorylated Hice1 species. Two neighboring nonspecific proteins (marked with asterisks) serve as loading controls.

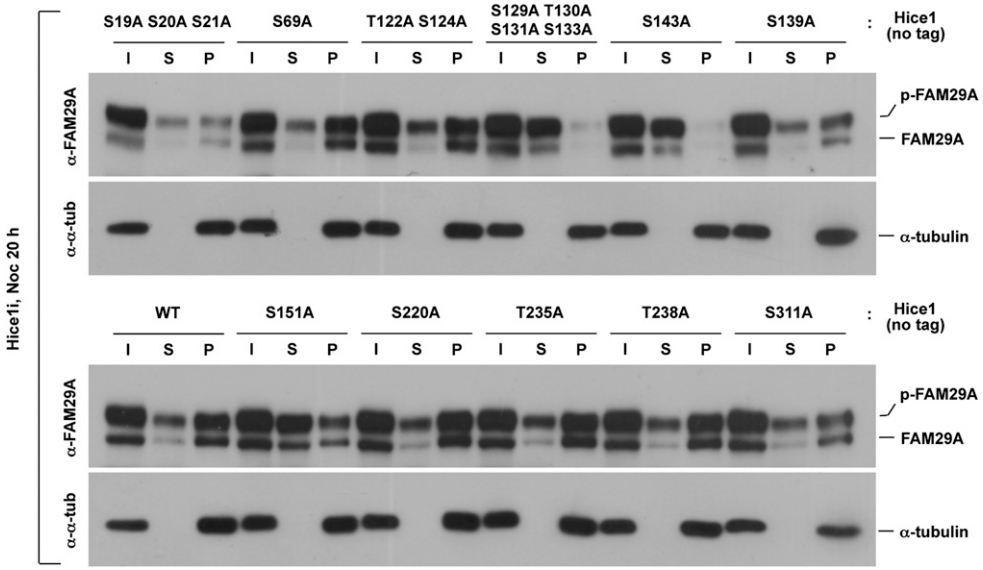

Fig. S5. Determination of Plk1-dependent phosphorylation sites on Hice1 critical for the Augmin–MT interaction. HeLa cells were first infected with lentivirus expressing either WT or various Hice1 mutants. After selection, the cells were depleted of the endogenous Hice1 by sh-Hice1 (Hice1i). The resulting cells were then arrested in mitosis by treating them with nocodazole for 20 h. Total lysates prepared from these cells were subjected to MT cosedimentation assays. Because of a high sensitivity of anti-FAM29A antibody, the ability of Hice1 mutants to bind to MT was assessed by examining the level of cosedimented FAM29A. The quadruple Hice1 mutant (129A, 130A, 131A, and 133A) and two single Hice1 mutants (143A and 151A) exhibited a significantly diminished ability to bind to MT.

Table S1. shRNA sequences used in this study

Target gene	Sequence (nucleotide positions from the start codon)	Source	Type
Luciferase	CGTACGCGGAATACTTCGA	(1)	Lentivirus
Hice1	GAACAATCTTGCTGAGTTT (492–510)	(2)	Lentivirus
Nedd1	GCAGACATGTGTCAATTTA(255–273)	(3)	Lentivirus
Plk1	AGATTGTGCCTAAGTCTCT (245–263)	(4)	Lentivirus

1. Elbashir SM, et al. (2001) Duplexes of 21-nucleotide RNAs mediate RNA interference in cultured mammalian cells. *Nature* 411:494–498.
2. Uehara R, et al. (2009) The augmin complex plays a critical role in spindle microtubule generation for mitotic progression and cytokinesis in human cells. *Proc Natl Acad Sci USA* 106: 6998–7003.
3. Lüders J, Patel UK, Stearns T (2006) GCP-WD is a gamma-tubulin targeting factor required for centrosomal and chromatin-mediated microtubule nucleation. *Nat Cell Biol* 8:137–147.
4. Hansen DV, Loktev AV, Ban KH, Jackson PK (2004) Plk1 regulates activation of the anaphase promoting complex by phosphorylating and triggering SCFbetaTrCP dependent destruction of the APC Inhibitor Emi1. *Mol Biol Cell* 15:5623–5634.

Table S2. Antibodies used in this study

Antibody	Species	Source
Anti-α-tubulin	Mouse	Sigma, St. Louis, MO
Anti-Cdc25C	Rabbit	Santa Cruz Biotechnologies, Santa Cruz, CA
Anti-Cdc27	Rabbit	Santa Cruz Biotechnologies, Santa Cruz, CA
Anti-Cyclin B1	Mouse	Santa Cruz Biotechnologies, Santa Cruz, CA
Anti-γ-tubulin	Mouse, Rabbit	Sigma, St. Louis, MO
Anti-ERK1, 2	Mouse	Cell Signaling Technology, Danvers, MA
Anti-Flag	Mouse	Clontech, Palo Alto, CA
Anti-FAM29A	Rabbit	Ryota Uehara and Gohta Goshima, Nagoya University, Nagoya, Japan
Anti-GFP	Mouse	Lab stock
Anti-GST	Mouse	Seung R. Kim, Chungbuk Natl. University, Cheongju, South Korea
Anti-Hice1	Rabbit	This study (Rockland Immunologicals, Gilbertsville, PA); GeneTex, Irvine, CA
Anti-Myc	Mouse	Lab stock
Anti-Nedd1	Rabbit	Jens Luders, Institute for Research in Biomedicine, Barcelona, Spain; Andreas Merdes, Centre Natl. de la Recherche Scientifique/Pierre Fabre, Toulouse, France; This study (Rockland Immunologicals, Gilbertsville, PA)
Anti-Nedd1 p-S460	Rabbit	This study (Epitomics, Inc., Burlingame, CA)
Anti-Plk1	Mouse	Santa Cruz Biotechnologies, Santa Cruz, CA
Anti-TPX2	Rabbit	Bethyl Laboratories, Montgomery, TX

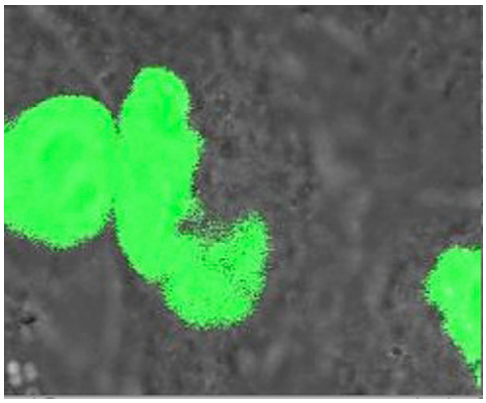

Movie S1. Normal mitotic progression observed in Nedd1 RNAi cells expressing RNAi-insensitive wild-type Nedd1. HeLa cells expressing WT Nedd1 were infected with lentivirus expressing EGFP-histone H2B. The resulting cells were then depleted of endogenous Nedd1 and arrested at the G1/S boundary by double-thymidine treatment. Eight hours after release from the G1/S block, cells were monitored under time-lapse microscopy. To better view the chromosome morphologies of the cells, EGFP fluorescence was artificially enhanced.

Movie S1

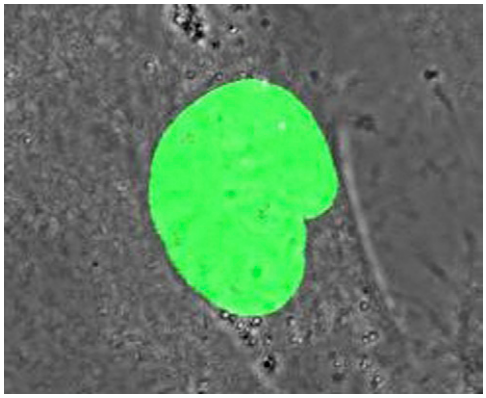

Movie S2. Generation of a micronucleated morphology in Nedd1 RNAi cells expressing an RNAi-insensitive Nedd1 S460A mutant. In this movie, a 460A mutant cell exhibits a significant preanaphase delay due to the presence of misaligned chromosomes and then displays a micronucleated chromosome morphology at later stages.

Movie S2

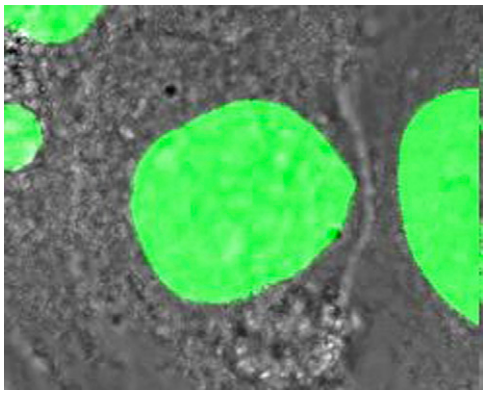

Movie S3. Generation of chromosome segregation defect in Nedd1 RNAi cells expressing an RNAi-insensitive Nedd1 S460A mutant. A S460A mutant cell exhibits a misaligned chromosome that later becomes a missegregating chromosome.

Movie S3

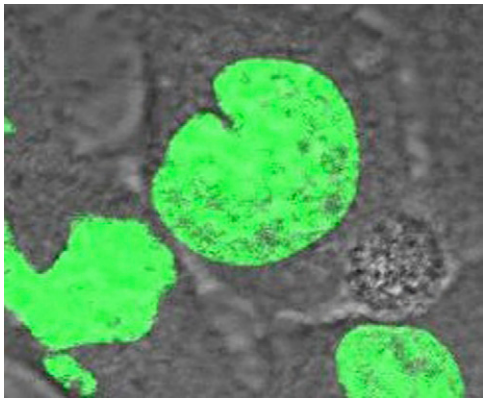

Movie S4. Induction of a prolonged mitotic arrest in Nedd1 RNAi cells expressing an RNAi-insensitive Nedd1 T550A mutant. A T550A mutant cell exhibits a prolonged preanaphase arrest due to the presence of misaligned chromosomes. Unlike the S460A mutant, micronucleated morphology was not easily observed in the T550A mutant.

Movie S4

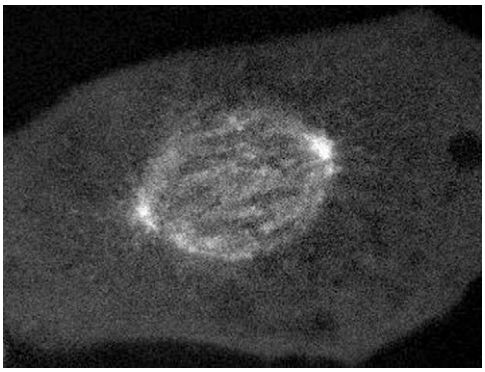

Movie S5. Requirement of normal Hice1 function in proper MT-based MT nucleation from within the spindle. The Hice1 RNAi (Hice1i) cells expressing an RNAi-insensitive WT Hice1 were infected with lentivirus expressing EB1–EGFP and then subjected to Zeiss VivaTome spinning disk microscopy.

Movie S5

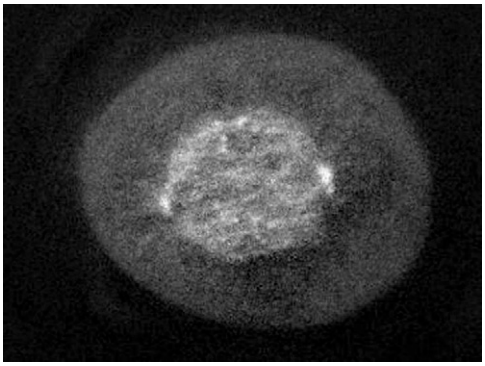

Movie S6. Rescue of the Hice1 RNAi defect in MT-based MT nucleation by the expression of a phosphomimic Hice1 6D mutant. An RNAi-insensitive Hice1 6D mutant was generated by mutating six Plk1-dependent phosphorylation sites on Hice1 to negatively charged Asp residues. The Hice1 RNAi (Hice1i) cells expressing Hice1 6D were infected with lentivirus expressing EB1–EGFP and then subjected to Zeiss VivaTome spinning disk microscopy.

Movie S6

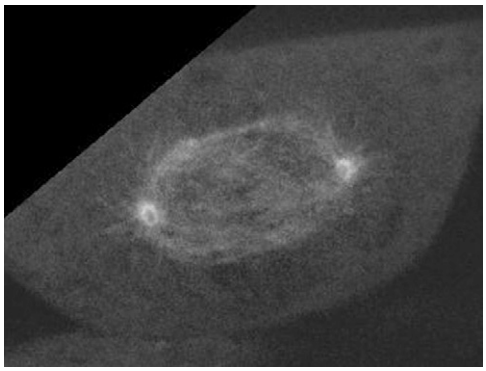

Movie S7. Requirement of Plk1-dependent Hice1 phosphorylation in proper MT-based MT nucleation. The Hice1 RNAi (Hice1i) cells expressing an RNAi-insensitive, Plk1-dependent Hice1 phosphosite mutant, Hice1 6A, were infected with lentivirus expressing EB1–EGFP and then subjected to Zeiss VivaTome spinning disk microscopy.

Movie S7

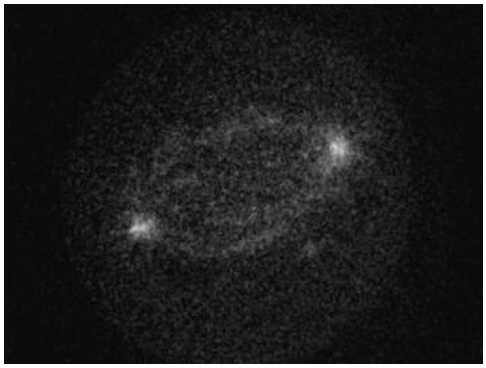

Movie S8. Defect associated with Hice1 RNAi in MT-based MT nucleation from within the spindle. The Hice1 RNAi (Hice1i) cells expressing control vector were infected with lentivirus expressing EB1–EGFP and then subjected to Zeiss VivaTome spinning disk microscopy.

Movie S8